NJC

Accepted Manuscript

This is an *Accepted Manuscript*, which has been through the Royal Society of Chemistry peer review process and has been accepted for publication.

Accepted Manuscripts are published online shortly after acceptance, before technical editing, formatting and proof reading. Using this free service, authors can make their results available to the community, in citable form, before we publish the edited article. We will replace this *Accepted Manuscript* with the edited and formatted *Advance Article* as soon as it is available.

You can find more information about *Accepted Manuscripts* in the Information for Authors.

Please note that technical editing may introduce minor changes to the text and/or graphics, which may alter content. The journal's standard Terms & Conditions and the Ethical guidelines still apply. In no event shall the Royal Society of Chemistry be held responsible for any errors or omissions in this *Accepted Manuscript* or any consequences arising from the use of any information it contains.

ROYAL SOCIETY OF CHEMISTRY

www.rsc.org/njc

Journal Name

ARTICLE

Enhanced performance of dye-sensitized solar cells with Y-shaped organic dyes containing di-anchoring groups

Received 00th January 20xx,
Accepted 00th January 20xx

DOI: 10.1039/x0xx00000x

www.rsc.org/

Hailang Jia,[a] Kang Shen,[a] Xuehai Ju,[b] Mingdao Zhang,[a] and Hegen Zheng*[a]

Two new Y-shaped D-π-$(A)_2$ type phenothiazine-based dyes (ZJA2 and ZJA3) were designed and synthesized for dye-sensitized solar cells (DSSCs). Compared to the single D-π-A analogue dye ZJA1, the Y-shaped dye with two carboxylic acid anchors was in favour of enhancing the performance of DSSCs. The FTIR spectra revealed that the dye ZJA2 molecules were anchored onto TiO_2 surface by two carboxylic acid anchors, which effectively increased the electron extraction channels. The steady-state emission spectra and time-resolved fluorescence experiments all indicated that the electron injection efficiency of dye ZJA2 was improved by the increased electron extraction channels, thus the J_{sc} of ZJA2 was greatly improved compared to dye ZJA1. In addition, the benzene was used as the π-bridge for linking di-anchoring groups, combined with CDCA, thereby reducing the charge recombination. As a result, the PCE of the DSSC based on ZJA2 (4.55%) was 67% higher than the DSSC based on ZJA1 (2.72%). The Y-shaped D-π-$(A)_2$ type phenothiazine-based dye ZJA3 containing two pyridine anchors was also investigated, the DSSC based on ZJA3 showed a poor PCE (0.45%) due to the low dye loading.

Introduction

Fossil energy crisis and environment pollution are common issues to the whole world, developing of renewable clean energy is one of the important means to solve this problem. Among the emerging photovoltaic technologies, dye-sensitized solar cells (DSSCs) have attracted significant attention due to their low costs and high power conversion efficiency (PCE).[1-4] Up to now, DSSCs have made remarkable progress and the highest PCE has reached 13% under AM 1.5G simulated sunlight illumination.[5] Efficient sensitizers can greatly improve the performance of DSSCs. Through years of research and development, many excellent sensitizers have been prepared, including ruthenium-complexes (N3 and N719),[6-8] zinc porphyrin dyes (YD2-O-C8 and SM315) and organic dyes (C219 and Y123).[9-14] Nevertheless, the performance of these sensitizers is greatly less than the ideal sensitizer. Thus, the improvement of sensitizer is still one of the most important researching directions to promote the development of DSSCs.[15]

It is well-known that most of the excellent sensitizers have the donor-π-acceptor (D-π-A) structures.[16,17] The special structure is associated with the efficient intra-molecular charge transfer (ICT) photoexcitation from donor (D) to acceptor (A), thus leading to efficient electron injection from the excited dye through anchoring group into the conduction band of the semiconductor. For an efficient dye, choose a maching anchoring group moiety is particularly important. The anchoring group determines the binding energy of the dye on TiO_2 and the electron injection rate.[18,19] Most of the D-π-A dyes use carboxylic aicd as the electron acceptor as well as the anchoring group for attachment on the TiO_2 surface. The carboxylic acid group can provide high electron injection rate for its good electronic coupling between dye and TiO_2 by forming a strong monodentate or bidentate linkage with Brønsted acid sites (surface bound hydroxyl groups, Ti-OH) on TiO_2 surface.[20-24] On the other hand, with the developmemnt of DSSCs, several new anchoring groups have been developed, such as pyridine, phosphonic acid and silyl.[25-29] But the single 1D-π-1A sensitizer often has a rod-shaped structure, which may cause undesirable dye aggregation and charge recombination. Because the 1D-π-1A type dye provides close π-π stacking of dye molecules which may lead to serious self-quenching of excited states and hence reduces the electron injection.[30,31] One of the effective strategies to solve this problem is employing multi-anchors for DSSCs. The dyes with multi-anchors for DSSCs can increase electron extraction channels and enhance binding strength, thereby suppressing the charge recombination and improving the performance of DSSCs.[32,33] In recent years, several efficient dyes containing double/multi anchoring groups have been reported and applied in DSSCs. Some literatures reported that the dyes with two acceptors/anchors (D-π-$(A)_2$) had better cell performance

[a] State Key Laboratory of Coordination Chemistry, School of Chemistry and Chemical Engineering, Collaborative Innovation Center of Advanced Microstructures, Nanjing University, Nanjing 210093, P. R. China, E-mail: zhenghg@nju.edu.cn. Fax: 86-25-83314502.
[b] School of Chemical Engineering, Nanjing University of Science and Technology, Nanjing 210094, P. R. China, E-mail: xhju@mail.njust.edu.cn
Electronic Supplementary Information (ESI) available: synthesis details and characterization data; Details for all physical characterizations. See DOI: 10.1039/x0xx00000x

than those with a single acceptor/anchor (D-π-A) due to improved photocurrent and stability.[34-39]

In this study, two Y-shaped D-π-$(A)_2$ type phenothiazine-based dyes (ZJA2 and ZJA3) were designed and synthesized. The single D-π-A phenothiazine-based dye (ZJA1) with mono-anchoring group was also prepared for comparison (Fig. 1). Two 9,9-dimethyl-9H-fluorene groups were introduced into the phenothiazine moiety as the donors (D), this stragety can effectively extend the π-conjugation and improve the photoresponse. The results indicated that the short-circuit current density (J_{sc}) of ZJA2 was greatly improved compared to ZJA1, due to the increased electron extraction channels and higher electron injection efficiency. We knew that benzene and heterocycle (thiophene or furan) have been widely used as the π-bridge linkers in many excellent dyes. In general, the benzene bridge results in a high open-circuit photovoltage (V_{oc}) compared to heterocycle. The main reason is that the benzene bridge can induce twist in the molecular planarity, thus reducing the charge recombination.[40] So we used benzene as the π-bridge for linking di-anchoring groups, in addition, chenodeoxycholic acid (CDCA) was also used to suppress the dye aggregation. Thus, the J_{sc} and V_{oc} of dye ZJA2 containing two carboxylic acid anchors were both improved compared to dye ZJA1 containing one carboxylic acid anchor. As a result, the PCE of the DSSC based on ZJA2 (4.55%) was superior to the DSSC based on ZJA1 (2.72%). We also investigated the difference between different anchoring groups (carboxylic acid and pyridine), the results indicated that the dye ZJA3 showed the poorest PCE (0.45%) due to the low dye loading.

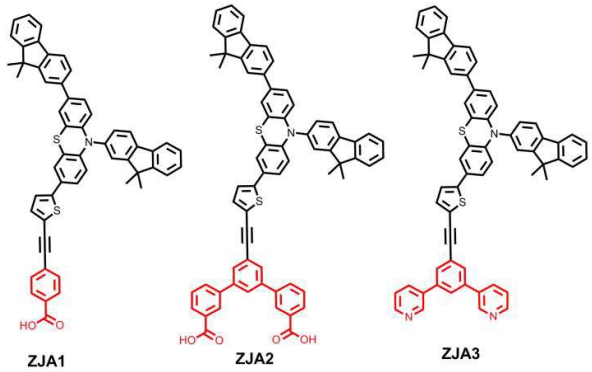

Fig. 1 Chemical structures of **ZJA1**, **ZJA2** and **ZJA3**

Experimental

General information

All solvents used were purified by standard methods, and all chemicals were purchased from commercial suppliers and used without further purification unless indicated otherwise. The ^{1}H NMR and ^{13}C NMR spectra were recorded on a Bruker DRX (500, 400 and 300 MHz) NMR spectrometer with tetramethylsilane (TMS) as the internal standard. The mass spectra were measured in ESI Mass Spectrometer (LCQ Fleet).

Synthesis and characterization of dyes

The synthetic routes of ZJA1, ZJA2 and ZJA3 are depicted in scheme 1. The synthesis details and characterization data (including ^{1}H NMR, ^{13}C NMR and ESI) are shown in supporting information.

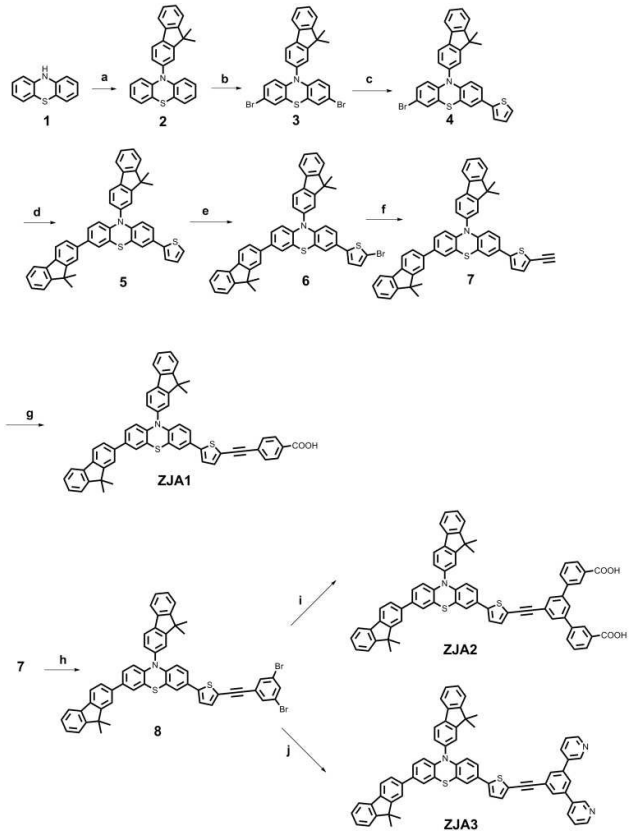

Scheme 1 Synthesis procedure of ZJA1, ZJA2 and ZJA3. Reagents and conditions: a) 2-bromo-9,9-dimethylfluorene, NaOBu-t, $Pd(OAc)_2$, $Pd(dppf)Cl_2$, toluene, 110℃; b) NBS, DMF, rt; c) 2-thiopheneboronic acid, $Pd(PPh_3)_4$, K_2CO_3, H_2O, 1, 4-dioxane, 90℃; d) 9,9-dimethyl-9H-fluoren-2-yl-boronic acid, $Pd(PPh_3)_4$, K_2CO_3, H_2O, 1, 4-dioxane, 90℃; e) NBS, DMF, rt; f) i: trimethylsilylacetylene, $Pd(PPh_3)_2Cl_2$, CuI, THF, TEA, 80℃; ii: K_2CO_3, CH_3OH, rt; g) i: ethyl 4-iodobenzoate, $Pd(PPh_3)_2Cl_2$, CuI, THF, TEA, 80℃; ii: NaOH, EtOH, H_2O, 90℃; h) tribromobenzene, $Pd(PPh_3)_2Cl_2$, CuI, THF, TEA, 80℃; i) i: 3-methoxycarbonylphenylboronic acid, $Pd(PPh_3)_4$, K_2CO_3, H_2O, 1, 4-dioxane, 90 ℃; ii: NaOH, EtOH, H_2O, 90℃; j) 3-pyridylboronic acid, $Pd(PPh_3)_4$, K_2CO_3, H_2O, 1, 4-dioxane, 90℃.

Fabrication of DSSCs

The photoanode (0.16 cm^2) was prepared by screen printing the TiO_2 paste on fluorine-doped tin oxide (FTO) glass plates (15 Ω / square). TiO_2 films (12 μm) consisting of a 8 μm transparent layer (particle size, 20 nm, pore size 32 nm) and a 4 μm scattering layer (200 nm particles). Before the screen printing process, the FTO glass plates were immersed in 40 mM $TiCl_4$ (aqueous) at 70℃ for 30 min and washed with water and ethanol. Then the TiO_2 films were performed with a programmed procedure: (1) heating at 80℃ for 15 min; (2) heating at 135℃ for 10 min; (3) heating at 325℃ for 30 min; (4) heating at 375℃ for 5 min; (5) heating at 450℃ for 15 min, and (6) heating at 500℃ for 15 min. Then the films were treated again with $TiCl_4$ at 70℃ for 30 min and sintered at

500℃ for 30 min. After cooling, the films were immersed into a solution of dye (0.5 mM) and CDCA (5 mM) in $CHCl_3$/EtOH (V/V, 1/1) for 18 h at room temperature. The photoanodes and the Pt counter electrode were sealed with a Surlyn film (25 μm) at 100℃. The electrolyte was introduced to the cells via pre-drilled holes in the counter electrode, the hole was sealed with a Surlyn film and a thin glass (0.1 mm thickness) cover by heating. Al foil was taped at the back side of each counter electrode to reflect the unadsorbed light. The electrolyte was composed of 0.6 M 1-butyl-3-methylimidazolium iodide (BMII), 30 mM I_2, 50 mM LiI, 0.5 M tert-butylpyridine and 0.1 M guanidiniumthiocyanate (GuNCS) in a solvent mixture of acetonitrile and valeronitrile (85:15, V/V).

Characterizations

The photocurrent-voltage (*J-V*) curves of the devices were measured on a Keithley 2400 source meter under an irradiance of 100 mW cm^{-2} at the surface of a testing cell by a xenon light source (Oriel). The incident photo-to-electron conversion efficiency (IPCE) spectra of the devices were measured by a DC method. The light source was a 300 W xenon lamp (Oriel 6258) coupled with a flux controller to improve the stability of the irradiance. The single wavelength was selected by a monochromator (Cornerstone 260 Oriel74125). Light intensity was measured by a NREL traceable Si detector (Oriel 71030NS) and the short circuit currents of the devices were measured by an optical power meter (Oriel 70310).

The UV-vis absorption spectra of dyes in DMF and dye-loaded films were recorded on a Shimadzu UV-3600 spectrometer. The fluorescence spectra were recorded on a Perkin Elmer LS55 spectrophotometer. The FTIR spectra were recorded on a Vector22 spectrometer. The time-resolved fluorescence lifetimes of the dyes in DMF and dye-loaded films were measured on a FLS920 spectrometer. Quasi-reversible oxidation and reduction waves were recorded on a Chenhua CHI660D model Electrochemical Workstation (Shanghai). Electrochemical Impedance Spectroscopy was studied using a Chenhua CHI660I model Electrochemical Workstation (Shanghai).

The dye loading were measured by a Shimadzu UV-3600 spectrometer. The sensitized 0.16 cm^2 electrodes were immersed into a 0.1 M NaOH solution in a mixed solvent (water/DMF = 1/1), which resulted in desorption of each dye.

Results and discussion

Synthesis

In this work, three new phenothiazine-based dyes (ZJA1, ZJA2 and ZJA3) were synthesized and applied in dye-sensitized solar cells. The structures of the three dyes and the synthetic route are shown in Fig. 1 and Scheme 1, respectively. The corresponding ^1H NMR, ^{13}C NMR and MS were also given in supporting information. We further studied the optical properties, electrochemical properties, electron injection dynamic and charge transfer processes.

Optical properties

The UV-vis absorption spectra of ZJA1, ZJA2 and ZJA3 in DMF are shown in Fig. 2 and the corresponding data are summarized in Table 1. The three dyes all have two major absorption bands in the range of 350-550 nm. The absorption band below 400 nm can be attributed to the π-π* transition of the conjugated molecules, and the absorption band in the range of 400-550 nm can be attributed to intramolecular charge transfer (ICT). They all exhibited high molar extinction coefficients (ε) in the visible absorption band, the ε of the three dyes reached $2.89\times10^4 M^{-1}cm^{-1}$ (ZJA1), $3.42\times10^4 M^{-1}cm^{-1}$ (ZJA2) and $2.64\times10^4 M^{-1}cm^{-1}$ (ZJA3), respectively. Especially for dye ZJA2, though it was slightly blue-shifted (3 nm) compared to dye ZJA1 (due to non-planar structure between the benzene and the two benzoic acid acceptors for ZJA2), but the ε of ZJA2 was about 1.2-fold higher than that of ZJA1. The absorption spectra of the three dyes anchored onto TiO_2 films were also investigated (Fig. 2b). We used CDCA as a coadsorbent to prevent dye aggregation on the TiO_2 surface. It was clear that the absorption peaks of the three dyes were all nearly no changed. The result indicated that the strategy successfully suppress dye aggregation on the TiO_2 surface, including two aspects of H-aggregation (blue-shift) and *J*-aggregation (red-shift) in adsorption. In addition, the spectra response of the three dyes anchored on the TiO_2 surface were all broadened. Especially for ZJA2 in the visible absorption band range, it exhibited significant enhancement compared to ZJA1. The result is in favour of improving the light-harvesting ability. The low absorption intensity of ZJA3 was mainly attribute to the low dye loading.

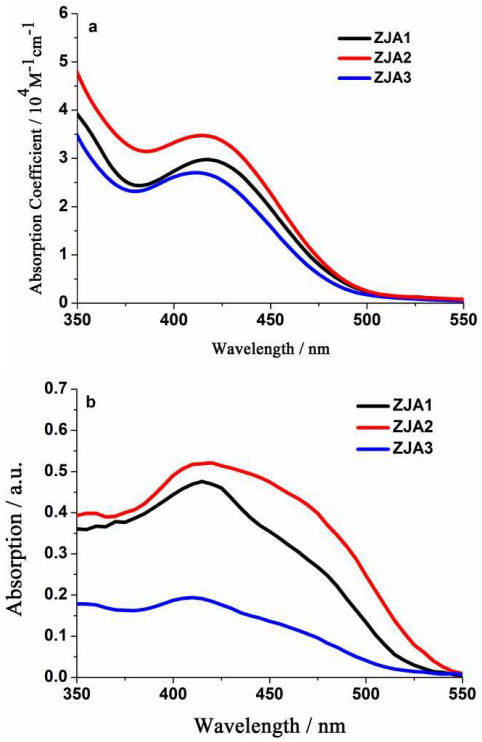

Fig. 2 (a) UV-Vis absorption spectra of **ZJA1**, **ZJA2** and **ZJA3** in DMF (b) Absorption spectra of **ZJA1**, **ZJA2** and **ZJA3** anchored on the 12 μm porous TiO_2 nanoparticle films.

Table 1 Optical and electrochemical properties of dyes

Dye	[a]λ_{max}/nm ($\varepsilon\times10^4 M^{-1}$ cm^{-1})	[b]λ_{max}/nm	[c]E_{OX}/V (*vs.* NHE)	[d]$E_{0\text{-}0}$/eV	[e]E_{Ox}^*/V (*vs.* NHE)	[f]HOMO/ LUMO(eV)
ZJA1	418(2.89)	555	1.07	2.33	-1.26	-5.47/-3.14
ZJA2	415(3.42)	556	1.03	2.31	-1.28	-5.43/-3.12
ZJA3	412(2.64)	558	1.09	2.36	-1.27	-5.49/-3.13

[a]Absorption maximum in DMF solution (1×10^{-6} M), [b]emission maximum in DMF solution (1×10^{-6} M), [c]E_{ox} potentials corresponding to the ground state oxidation potentials, [d]$E_{0\text{-}0}$ was estimated from the UV-vis absorption onset, [e]E_{ox}^* was calculated by the formula: $E_{ox}^* = E_{ox}-E_{0\text{-}0}$, [f]HOMO and LUMO energies were calculated using formula HOMO (*vs.* NHE)=-[eE_{ox} (*vs.* NHE)+4.4eV], LUMO=-($E_{0\text{-}0}$-HOMO).[23,41]

Electrochemical properties

The electrochemical properties of dyes are very important for DSSCs, which can effect on the ability of electron injection from the excited dyes into the conduction band of TiO_2 and the dye regeneration. The cyclic voltammograms of the dyes are shown in Fig. S2 and the corresponding data are summarized in Table 1. As shown in Table 1, the ground state oxidation potentials (E_{ox}) of the dyes are 1.07 V (ZJA1), 1.03 V (ZJA2) and 1.09 V (ZJA3), respectively. They are all more positive than the redox potential of the I^-/I_3^- redox couple (0.4V vs. NHE), ensuring an efficient driving force to achieve regeneration from the oxidized dyes. The zero-zero excitation energy ($E_{0\text{-}0}$) was estimated from the absorption onset. The $E_{0\text{-}0}$ values of the dyes are 2.33 eV (ZJA1), 2.31 eV (ZJA2) and 2.36 eV (ZJA3), respectively. The excited oxidation potentials (E_{ox}^*) of the three dyes are -1.26 V (ZJA1), -1.28 V (ZJA2) and -1.27 V (ZJA3), respectively. They are all more negative than the Fermi level of TiO_2 (-0.5 V vs. NHE), which suggest that the electron from the excited dyes can effectively inject into the conduction band of TiO_2.[42]

The anchoring modes analysis

In order to investigate the adsorption states of the three dyes on TiO_2 films, we measured the FTIR spectra of the dye powders and the dyes adsorbed on TiO_2 films (Fig. S3). For powder of dye ZJA1, the carbonyl peak was found at 1688 cm^{-1}, disappeared after anchoring on TiO_2 film. And a new band appeared at 1624 cm^{-1}, which represented the antisymmetric stretching $\nu(COO_{as}^-)$.[43,44] This observation indicates that dye ZJA1 adsorbs at the TiO_2 surface via dehydration reactions. For powder of D-π-$(A)_2$ dye ZJA2, the carbonyl peak was found at 1692 cm^{-1}. After anchored on TiO_2 surface, the carbonyl peak disappeared completely. As well as dye ZJA1, a new band appeared at 1627 cm^{-1}, which also represented the antisymmetric stretching $\nu(COO_{as}^-)$. The result suggests that the D-π-$(A)_2$ dye was chemically adsorbed on TiO_2 surface *via* di-anchoring mode. Dye ZJA3 containing two pyridine anchors was also measured. For powder of dye ZJA3, the characteristic stretching bands for C=N or C=C were observed at 1598 cm^{-1}, 1476 cm^{-1} and 1446 cm^{-1}. After anchored on TiO_2 surface, a new band appeared at 1616 cm^{-1}, which can be assigned to pyridine anchor coordinated to the Lewis acid sites of the TiO_2 surface.[25,26]

Photovoltaic performance of DSSCs

Table 2 Photovoltaic parameters of the DSSCs obtained from the *J-V* curves

Dye	J_{sc} (mA cm^{-2})	V_{oc} (mV)	FF (%)	η (%)	Dye loading (10^{-7} mol cm^{-2})
ZJA1	6.45±0.05	656±2.00	64.3±0.32	2.72±0.01	2.13
ZJA2	9.62±0.06	704±4.40	67.1±0.32	4.55±0.01	3.24
ZJA3	2.21±0.08	527±1.60	38.4±0.97	0.45±0.02	0.38

The DSSCs were measured under AM 1.5G irradiation, the effective areas of all DSSCs were 0.16 cm^2, the photoanode was immersed in a solution of the dyes (0.5 mM) and CDCA (5 mM) in $CHCl_3$/EtOH (V/V, 1/1) for 18 h at room temperature.

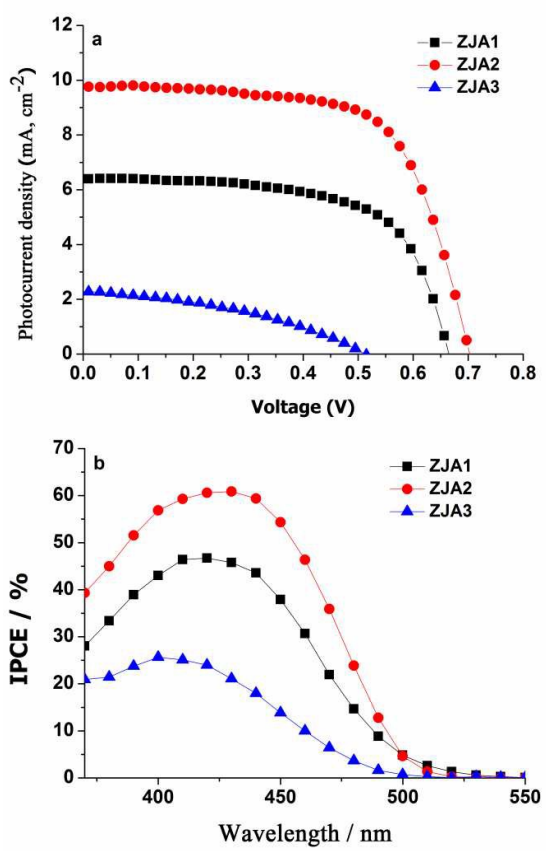

Fig. 3 (a) The *J-V* curves of DSSCs based on **ZJA1**, **ZJA2** and **ZJA3**, (b) The IPCE curves of DSSCs based on **ZJA1**, **ZJA2** and **ZJA3**.

The photovoltaic performance of the DSSCs based on the three dyes under AM 1.5G irradiation have been investigated (Fig. 3), and the corresponding parameters were collected in Table 2. As shown in Fig. 3a, the current density-voltage (*J-V*) curve of DSSC based on ZJA1 exhibited a short-circuit current density (J_{sc}) of 6.45 mA cm^{-2}, an open-circuit photovoltage (V_{oc}) of 656 mV and a fill factor (FF) of 64.3%, generating a PCE of 2.72%. It is worth noting that the performance of DSSC based on ZJA2 was greatly improved compared to the DSSC based on ZJA1. Through introducing two carboxylic acid anchors by the benzene bridge for dye ZJA2, the PCE of DSSC based on ZJA2 (4.55%) is about 67% higher than that of DSSC based on ZJA1. The J_{sc} (9.62 mA cm^{-2}) and V_{oc} (704 mV) of DSSC based on ZJA2 were both much higher than those of DSSC based on ZJA1. The resuts suggest that it is an effective strategy to improve the performance of DSSC by introduing di-anchoring groups through the benzene bridge. The DSSC based on ZJA3 exhibited a poor PCE of 0.45%, the J_{sc}, V_{oc} and FF were all very

low, the main reason is attribute to the low dye loading. The values of dye loading for ZJA1 and ZJA2 are 2.13×10^{-7}mol cm^{-2} and 3.24×10^{-7}mol cm^{-2}, respectively. In contrast, the value of dye loading for ZJA3 is only 0.38×10^{-7}mol cm^{-2}. The incident photo-to-electron conversion efficiency (IPCE) spectra of DSSC based on the three dyes were also investigated, as shown in Fig. 3b. It is easy to find that ZJA2 shows a higher value than the other two dyes. The IPCE value of DSSC based on ZJA2 is more than 50% in the region of 387-455 nm and with a maximum value of 60.7% at 423 nm, while the maximum values of ZJA1 and ZJA3 are 46.6% and 25.2%, respectively. The result is consistent with J_{sc} of the DSSCs. We also measured the light-harvesting efficiency (LHE) of the dyes on TiO_2 films (Fig. S4). The result is consistent with IPCE of the DSSCs.[45-47]

Table 3 Fitting parameter (χ^2) and excited-state lifetime (τ) from the fluorescence decay curves

Dye	χ^2	τ (ns)
ZJA1-DMF	1.06	2.73
ZJA1-TiO_2	1.05	0.67
ZJA2-DMF	1.05	3.57
ZJA2-TiO_2	1.07	0.41
ZJA3-DMF	1.01	3.47
ZJA3-TiO_2	1.10	0.49

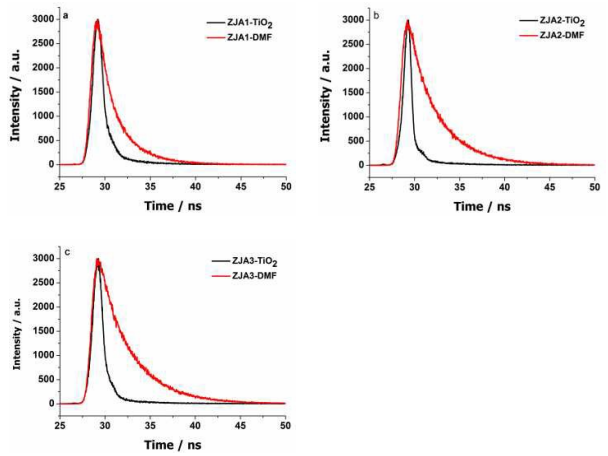

Fig. 4 Fluorescence decay curves of dyes in DMF (red line) and dyes adsorbed onto the TiO_2 surface (black line), (a)**ZJA1**, (b)**ZJA2**, (c)**ZJA3**.

The electron injection dynamic studies

The time-resolved fluorescence experiments and steady-state fluorescence experiments on ZJA1, ZJA2 and ZJA3 were measured to investigate the difference in the electron injection dynamic of the three dyes. Fig. 4 shows the time-resolved luminescence of the two dyes in DMF and adsorbed on TiO_2, and the corresponding data are summarized in Table 3.[5,9,11] In DMF, the fluorescence lifetime values of ZJA1, ZJA2 and ZJA3 are 2.73 ns, 3.57 ns and 3.47 ns, respectively. It is clear that the excited-state lifetimes of ZJA2 and ZJA3 are both longer than that of ZJA1. When the three dyes adsorbed on TiO_2 films, the fluorescence of the three dyes decayed rapidly. On the TiO_2 films, the fluorescence lifetime values of ZJA1, ZJA2 and ZJA3 are 670 ps, 410 ps and 490 ps, respectively. Compared to ZJA1, the emission decay of ZJA2 and ZJA3 were both further enhanced, especially for ZJA2. The results indicated that the excited charge transfer from ZJA2 to the conduction band of TiO_2 may be more effective than that in the case of ZJA1. We further carried out the steady-state fluorescence experiments to confirm the inference (Fig. S5). Because the excited-state injection can not occur onto Al_2O_3, so the excited-state properties for the three dyes were evaluated on Al_2O_3. When the three dyes adsorbed on TiO_2, fluorescence from ZJA1 and ZJA3 was quenched about 78% and 82%, respectively, while the fluorescence from ZJA2 was quenched about 92% relative to ZJA2-Al_2O_3. This suggests that the injection quantum yield of ZJA2 and ZJA3 are both higher than that of ZJA1.[48] Thus, the electron injection efficiency of the dye containing di-anchoring groups was improved.

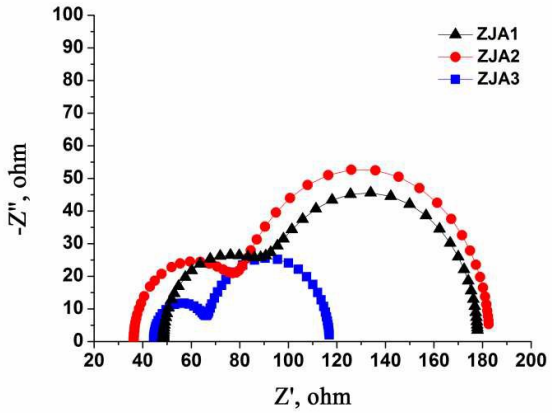

Fig. 5 Nyquist plots of the DSSCs based on **ZJA1, ZJA2** and **ZJA3.**

The charge recombination process studies

Electrochemical impedance spectroscopy (EIS) is a very useful tool for DSSC. Many researchers often used it to investigate the interfacial charge recombination process under dark conditions.[49,50] The EIS of the DSSCs based on the three dyes were measured at an applied voltage of -0.6 V, and scanned from 10^5 to 1 Hz. The Nyquist plots are shown in Fig .5 and we can see two semicircles in the plots. We know that the large semicircle represents the charge recombination process at the TiO_2/dye/electrolyte interface, and the small semicircle represents the charge transport at the Pt/electrolyte interface. The radius of the large semicircle corresponds to the charge recombination resistance (R_{rec}). The larger charge recombination resistance value stands for lower charge recombination rate. Obviously, with the same electrode materials and the same electrolyte, the DSSC based on ZJA2 showed the largest R_{rec}. The result indicated that dye ZJA2 with two carboxylic acid anchors can more effectively reduce charge recombination than dye ZJA1 with single carboxylic acid anchor. The R_{rec} result is also consistent with the V_{oc} of the DSSCs. As shown in Fig. S6, we infer that the large twist angles between the benzene bridge and the two benzoic acid acceptors (about 37°) may block the penetration of the electrolyte through the dye forest. This is helpful to reduce the charge recombination, similar to the previous reports in the literatures.[37,40]

Conclusions

In summary, two new Y-shaped phenothiazine-based dyes (ZJA2 and ZJA3) containing di-anchoring groups were synthesized and applied in dye-sensitized solar cells (DSSCs). Compared to the single D-π-A analogue dye ZJA1, the PCE of DSSC based on ZJA2 (4.55%) was about 67% higher than that of DSSC based on ZJA1 (2.72%). The results indicated that introduced two carboxylic acid anchors by the benzene bridge in the design of sensitizers can effectively improve the performance of DSSCs. This work presents a new strategy to designing efficient dye with improved electron injection efficiency and reduced charge recombination toward high-performance DSSCs.

Acknowledgements

This work was supported by grants from the National Natural Science Foundation of China (Nos. 21371092; 21401107), National Basic Research Program of China (2010CB923303), Natural Science Foundation of Jiangsu Province, China (No. BK20140986).

Notes and references

1 B. O'Regan, M. Grätzel, *Nature*, 1991, **353**, 737.
2 M.-E. Ragoussia, T. Torres, *Chem. Commun.*, 2015, **51**, 3957.
3 G. Calogero, A. Bartolotta, G. D. Marco, A. D. Carlob and F. Bonaccorso, *Chem. Soc. Rev.,* 2015, **44**, 3244.
4 L. L. Li, E. W. G. Diau, *Chem. Soc. Rev.,* 2013, **42**, 291.
5 S. Mathew, A. Yella, P. Gao, R. Humphry-Baker, B. F. E. Curchod, N. Ashari-Astani, I. Tavernelli, U. Rothlisberger, M. K. Nazeeruddin and M. Grätzel, *Nature Chemistry*, 2014, **6**, 242.
6 M. K. Nazeeruddin, A. Kay, I. Rodicio, R. Humpbry-Baker, E. Miiller, P. Liska, N. Vlachopoulos and M. Grätzel, *J. Am. Chem. Soc.*, 1993, **115**, 6382.
7 M. K. Nazeeruddin, F. D. Angelis, S. Fantacci, A. Selloni, G. Viscardi, P. Liska, S. Ito, B. Takeru and M. Grätzel, *J. Am. Chem. Soc.*, 2005, **127**, 16835.
8 Q. J. Yu, Y. H. Wang, Z. H. Yi, N. N. Zu, J. Zhang, M. Zhang and P. Wang, *Acs, Nano.*, 2010, **4**, 6032.
9 A. Yella, H. W. Lee, H. N. Tsao, C. Yi, A. K. Chandiran, M. K. Nazeeruddin, E. W. G. Diau, C. Y. Yeh, S. M. Zakeeruddin and M. Grätzel, *Science*, 2011, **334**, 629.
10 T. Higashinoa, H, Imahori, *Dalton Trans*, 2015, **44**, 448.
11 A. Yella, C.-L. Mai, S. M. Zakeeruddin, S.-N. Chang, C.-H. Hsieh, C.-Y. Yeh and M. Grätzel, *Angew. Chem. Int. Ed.*, 2014, **53**, 2973.
12 W. Zeng, Y. Cao, Y. Bai, Y. Yang, Y. Shi, M. Zhang, F. Wang, C. Pan and P. Wang, *Chem. Mater.*, 2010, **22**, 1915.
13 H. N. Tsao, C. Yi, T. Moehl, J.-H. Yum, S. M. Zakeeruddin, M. K. Nazeeruddin and M. Grätzel, *ChemSusChem*, 2011, **4**, 591.
14 H. Zhu, Y. Wu, J. Liu, W. Zhang, W. Wu and W.-H. Zhu, *J. Mater. Chem. A*, 2015, **3**, 10603.
15 C.-P. Lee, R. Y.-Y. Lin, L.-Y. Lin, C.-T. Li, T.-C. Chu, S.-S. Sun, J. T. Lin and K.-C. Ho, *RSC Adv.*, 2015, **5**, 23810.
16 X. Zhang, J. Mao, D. Wang, X. Li, J. Yang, Z. Shen, W. Wu, J. Li, H. Ågren and J. Hua, *ACS Appl. Mater. Interfaces*., 2015, **7**, 2760.
17 C.-L. Wang, J.-Y. Hu, C.-H. Wu, H.-H. Kuo, Y.-C. Chang, Z.-J. Lan, H.-P. Wu, E. W.-G. Diau and C.-Y. Lin, *Energy Environ. Sci.*, 2014, **7**, 1392.
18 L. Zhang, J. M. Cole, *ACS Appl. Mater. Interfaces*, 2015, **7**, 3427.
19 F. Ambrosio, N. Martsinovich, A. Troisi, *J. Phys. Chem. Lett*, 2012, **3**, 1531.
20 B. L. Watson, B. D. Sherman, A. L. Moore, T. A. Moore and D. Gust, *Phys. Chem. Chem. Phys*, 2015, **17**, 15788.
21 D. Joly, L. Pelleja, S. Narbey, F. Oswald, T. Meyer, Y. Kervella, P. Maldivi, J. N. Clifford, E. Palomares and R. Demadrille, *Energy Environ. Sci*., 2015, **8**, 2010.
22 X. Qian, W.-Y. Chang, Y.-Z. Zhu, S.-S. Wang, B. Pan, L. Lu and J.-Y. Zheng, *RSC Adv*., 2015, **5**, 47422.
23 L. Cabau, C. V. Kumar, A. Moncho, J. N. Clifford, N. Lopeza and E. Palomares, *Energy Environ. Sci*., 2015, **8**, 1368.
24 C.-L. Wang, J.-W. Shiu, Y.-N. Hsiao, P.-S. Chao, E. W.-G. Diau and C.-Y. Lin, *J. Phys. Chem. C,* 2014, **118**, 27801.
25 G. Alemu, J. Cui, K. Cao, J. Li, Y. Shen and M. Wang, *RSC Adv*., 2014, **4**, 51374.
26 Y. Ooyama, N. Yamaguchi, I. Imae, K. Komaguchi, J. Ohshita and Y. Harima, *Chem. Commun.*, 2013, **49**, 2548.
27 K. Kakiage, Y. Aoyama, T. Yano, K. Oya, T. Kyomen and M. Hanaya, *Chem. Commun.*, 2015, **51**, 6315.
28 K.-C. Liao, H. Anwar, I. G. Hill, G. K. Vertelov and J. Schwartz, *ACS Appl. Mater. Interfaces*., 2012, **4**, 6735.
29 E. Gabrielsson, H. Tian, S. K. Eriksson, J. Gao, H. Chen, F. Li, J. Oscarsson, J. Sun, H. Rensmo, L. Kloo, A. Hagfeldt and L. Sun, *Chem. Commun.*, 2015, **51**, 3858.
30 B. G. Kim, K. Chung, J. Kim, *Chem. Eur. J.*, 2013, **19**, 5220.
31 X. Lu, X. Jia, Z.-S. Wang and G. Zhou, *J. Mater. Chem. A*, 2013, **1**, 9697.
32 N. Manfredi, B. Cecconi and A. Abbotto, *Eur. J. Org. Chem.,* 2014, 7069.
33 X. Qian, H.-H. Gao, Y.-Z. Zhu, L. Lu and J.-Y. Zheng, *RSC Adv*., 2015, **5**, 4368.
34 Y.-F. Chen, J.-M. Liu, J.-F. Huang, L.-L. Tan, Y. Shen, L.-M. Xiao, D.-B. Kuang and C.-Y. Su, *J. Mater. Chem. A*, 2015, **3**, 8083.
35 A. Abbotto, N. Manfredi, C. Marinzi, F. D. Angelis, E. Mosconi, J.-H. Yum, X. Zhang, M. K. Nazeeruddin and Michael Grätzel, *Energy Environ. Sci*., 2009, **2**, 1094.
36 J. Liu, J. Zhang, M. Xu, D. Zhou, X. Jing and P. Wang, *Energy Environ. Sci*., 2011, **4**, 3021.
37 R. Y.-Y. Lin, F.-L. Wu, C.-H. Chang, H.-H. Chou, T.-M. Chuang, T.-C. Chu, C.-Y. Hsu, P.-W. Chen, K.-C. Ho, Y.-H. Loc and J. T. Lin, *J. Mater. Chem. A*, 2014, **2**, 3092.
38 C.-H. Siu, L. T. L. Lee, P.-Y. Ho, P. Majumdar, C.-L. Ho, T. Chen, J. Zhao, H. Lie and W.-Y. Wong, *J. Mater. Chem. C*, 2014, **2**, 7086.
39 D. Heredia, J. Natera, M. Gervaldo, L. Otero, F. Fungo, C.-Y. Lin and K.-T. Wong, *Org. Lett.,* 2010, **12**, 12.
40 H. Zhu, B. Liu, J. Liu, W. Zhang and W.-H. Zhu, *J. Mater. Chem.* C, 2015, **3**, 6882.
41 J.-S. Ni, J.-H. You, W.-I. Hung, W.-S. Kao, H.-H. Chou and J. T. Lin, *ACS Appl. Mater. Interfaces*., 2014, **6**, 22612.
42 S. H. Kim, H. W. Kim, C. Sakong, J. Namgoong, S. W. Park, M. J. Ko, C. H. Lee, W. I. Lee and J. P. Kim, *Org. Lett.,* 2011, **13**, 5784.
43 S. Wenger, P.-A. Bouit, Q. Chen, J. Teuscher, D. D. Censo, R. Humphry-Baker, J.-E. Moser, J. L. Delgado, N. Martin, S. M. Zakeeruddin and M. Grätzel, *J. Am. Chem. Soc.*, 2010, **132**, 5164.
44 S. E. Brown-Xu, M. H. Chisholm, C. B. Durr, T. L. Gustafson and T. F. Spilker, *J. Am. Chem. Soc.*, 2014, **136**, 11428.
45 Y. Cakmak, S. Kolemen, M. Buyuktemiz, Y. Dede and S. Erten-Ela, *New J. Chem.,* 2015, **39,** 4086.
46 A. Fillinger, B. A. Parkinson, *Journal of the Electrochemical Society*, 1999, **146,** 4559.
47 J. Mao, N. He, Z. Ning, Q. Zhang, F. Guo, L. Chen, W. Wu, J. Hua and H. Tian, *Angew. Chem. Int. Ed.*, 2012, **51**, 9873.

48 A. Nayak, R. R. Knauf, K. Hanson, L. Alibabaei, J. J. Concepcion, D. L. Ashford, J. L. Dempsey and T. J. Meyer, *Chem. Sci*., 2014, **5**, 3115.
49 F. M. Jradi, X Kang, D. O'Neil, G. Pajares, Y. A. Getmanenko, P. Szymanski, T. C. Parker, M. A. El-Sayed and S. R. Marder, *Chem. Mater.*, 2015, **27**, 2480.
50 G. Wang, Y. Wu, W. Ding, G. Yu, Z. Hu, H. Wang, S. Liu, Y. Zou and C. Pan, *J. Mater. Chem. A*, 2015, **3**, 14217.

Table of contents entry

Introducing two carboxylic acid anchors by the benzene bridge in the design of sensitizers can effectively improve the performance of DSSCs.